Theoretical Calculation of the Dehydrogenation of Ethanol on a $Rh/CeO_2(111)$ Surface

Hui-Lung Chen, Shih-Hung Liu, and Jia-Jen Ho*

Department of Chemistry, National Taiwan Normal University, 88, Section 4, Tingchow Road, Taipei 116, Taiwan

Received: February 17, 2006; In Final Form: June 2, 2006

We applied periodic density-functional theory (DFT) to investigate the dehydrogenation of ethanol on a Rh/CeO_2 (111) surface. Ethanol is calculated to have the greatest energy of adsorption when the oxygen atom of the molecule is adsorbed onto a Ce atom in the surface, relative to other surface atoms (Rh or O). Before forming a six-membered ring of an oxametallacyclic compound ($Rh-CH_2CH_2O-Ce_{(a)}$), two hydrogen atoms from ethanol are first eliminated; the barriers for dissociation of the O−H and the β-carbon (CH_2-H) hydrogens are calculated to be 12.00 and 28.57 kcal/mol, respectively. The dehydrogenated H atom has the greatest adsorption energy (E_{ads} = 101.59 kcal/mol) when it is adsorbed onto an oxygen atom of the surface. The dehydrogenation continues with the loss of two hydrogens from the α-carbon, forming an intermediate species $Rh-CH_2CO-Ce_{(a)}$, for which the successive barriers are 34.26 and 40.84 kcal/mol. Scission of the C−C bond occurs at this stage with a dissociation barrier E_a = 49.54 kcal/mol, to form $Rh-CH_{2(a)} + 4H_{(a)} + CO_{(g)}$. At high temperatures, these adsorbates desorb to yield the final products $CH_{4(g)}$, $H_{2(g)}$, and $CO_{(g)}$.

Introduction

Catalytic converters have been intensively studied in relation to new sources to generate low-emission power, such as solid-oxide fuel cells.[1,2] Ceria (CeO_2) has emerged as an important promoter of heterogeneous catalytic reactions;[3,4] in automotive systems to control gaseous emissions, ceria is a crucial component of the "three-way catalysts" that simultaneously convert hydrocarbons, CO and NO_x, present in the exhaust, into H_2O, CO_2, and N_2.[5−7] The capacity of ceria to store oxygen (oxygen storage capacity, OSC, the ability to act as an oxygen buffer) makes this material an important ingredient in these converters.[8−10] It is also an important catalyst for the oxidation of CO[11] and hydrocarbons[12] and the decomposition of alcohols[13] and aldehydes.[14] Hydrogen is considered a desirable fuel for several reasons, among which hydrogen is the least polluting fuel that one can use in an internal-combustion engine, and it can serve in a highly efficient hydrogen/oxygen fuel cell to produce electricity.[15−17] Because hydrogen is hardly found on earth in its most usable form, the synthesis of hydrogen becomes essential.

In papers about the reaction of ethanol on surfaces of M/ceria catalysts with M = Pd, Pt, Rh, Au, Pt−Pd, Au−Rh, and Pt−Rh, Idriss et al.[18−22] made several observations. (1) The adsorption of ethanol on Rh/CeO_2, $Au-Rh/CeO_2$, and $Pt-Rh/CeO_2$ leads directly to scission of the carbon−carbon bond. (2) To the extent of reduction of CeO_2 (ΔO) for a series containing various metals, Rh had the least ΔO value. (3) The addition of Rh into CeO_2 greatly destabilizes acetaldehyde, likely due to a direct interaction between Rh and an ethoxide species in an oxametallacyclic conformation, shown in Scheme 1. (4) The production of hydrogen from ethanol involves the breaking of a carbon−carbon bond, and Rh/CeO_2 appears to be the most suitable compound for this purpose at accessible operating temperatures. With regard to the interaction between Rh and CeO_2, Imamura et al.[23] reported that no transmission electron microscope (TEM) image of Rh was obtained on CeO_2 prepared upon calcination at 550 °C. Electron spectroscopy for chemical analysis (ESCA) and X-ray diffraction (XRD) analyses revealed that Rh penetrated into the ceria so that only a small proportion remained on the surface. They found Rh, however, present as metallic particles on a ceria surface calcined at 950 °C. Although the proportion of Rh exposed on the surface of ceria was small, the Rh in this state was highly active in decomposing ethanol.

SCHEME 1: Formation and Structure of an Oxametallacycle on Rh/CeO_2 Catalysts[a]

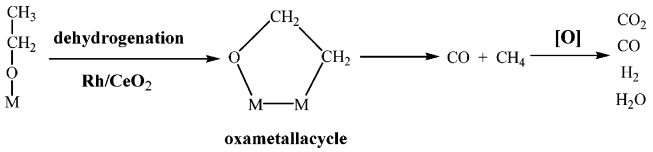

[a] [O] denotes surface oxygen and M denotes a metal or a Ce ion site.

In principle, hydrogen can be extracted from any hydrocarbon, such as methanol, natural gas, and motor fuel. These sources that are derived from fossil fuels suffer from a major drawback: they do not decrease a reliance on fossil fuels and they still emit pollutants and greenhouse gases (CO_2).[24] For its relatively large hydrogen content, availability, nontoxicity, and safety of storage and handling, a feasible alternative is bioethanol. Production of ethanol from sugar- or starch-containing crops (green field) is a well-established industrial technique that has been practiced for many years.[25] The use of ethanol derived from biomass to produce hydrogen and energy has a great potential for significant contributions toward environmental protection. Production of hydrogen from ethanol via steam reforming or catalytic partial oxidation has been shown to be entirely feasible from a thermodynamic point of view,[26−28] and several catalysts have been proposed that show sufficient activity and stability to be considered further for practical applications.[29−35]

* To whom correspondence should be addressed. E-mail: jjh@ntnu.edu.tw. Tel: (886)-2-29309085. Fax: (886)-2-29324249.

10.1021/jp0610259 CCC: $33.50
Published on Web 07/13/2006

TABLE 1: Optimized Bond Lengths and Adsorption Energies[a], E_{Ads} (kcal/mol), for CH_3CH_2OH and Its Fragments on the $Rh/CeO_2(111)-(2 \times 1)$ Surface, Calculated by the Slab Model Using VASP (optimized structures are shown in Figure 2)

species	r(Ce(O)−O(H))	r(Rh−C(O,H))	r(C−C(O))	E_{ads}
$CH_3CH_2O(H)-Ce(a)$	2.64		1.51	13.95
$CH_3CH_2O(H)-Rh(a)$		2.64	1.51	9.37
$CH_3CH_2O-Ce(a)$	2.22		1.54	64.68
$CH_3CH_2O-Rh(a)$		2.24	1.54	61.81
$Rh-CH_2CH_2O-Ce(a)$	2.61	2.06	1.55	40.25
$Rh-CH_2CHO-Ce(a)$	2.81	2.16	1.42	77.71
$Rh-CH_2CO-Ce(a)$	2.81	2.11	1.49	50.18
$Rh-CHCO-Ce(a)$	3.06	2.01	1.41	89.80
$H_2CO-Ce(a)$	2.90		1.25	20.85
$HCO-Ce(a)$	2.89		1.04	27.33
$CO-Ce(a)$	3.23		1.15	3.55
$H_2C-Rh(a)$		1.80		92.13
$H-Ce(a)$	2.18			28.52
$H-Rh(a)$		1.59		56.25
$H-O(a)$	0.97			101.59

[a] $E_{ads} = -(E_{total} - E_{molecule} - E_{surface})$.

Theoretical calculations of properties of a CeO_2 surface, such as energetics, surface relaxation, and electronic structure, have been performed;[36−40] the sequence of stability of the studied surfaces was (111) > (110) > (100), in agreement with experimental observations [41] employing X-ray photoelectron spectroscopy (XPS) and low-energy electron diffraction (LEED) techniques. Although some theoretical investigations on stoichiometric bulk ceria are available in the literature, there seems to exist no theoretical investigation of the adsorption and dehydrogenation of ethanol on the surface of Rh/CeO_2: the interaction mechanisms have thus yet to be adequately addressed theoretically. Here, we present a systematic, periodic, self-consistent, density-functional theoretical (DFT) calculation of possible pathways for dehydrogenation of ethanol on a Rh/CeO_2-$(111)-(2 \times 1)$ surface. We address both the adsorbed intermediates and the reaction barriers in the pathways and present also the possible potential-energy surfaces.

Computational Method

We applied plane-wave periodic density-functional theoretical calculations implemented in the Vienna ab initio simulation program (VASP).[42−44] The generalized gradient approximation (GGA) [45] of Perdew and Wang (PW91) [46] was used for the exchange-correlation functional. Here, we employ Blochl's all-electron (with frozen core) projector augmented wave (PAW) method[47a] as implemented by Kresse and Joubert.[47b] Tight convergence of the plane-wave expansion was obtained with a moderate truncation energy 900 eV, while the electronic relaxation is terminated with a change in the total free energy smaller than 1×10^{-4} eV. A Monkhorst pack[48] scheme served in the generation of the k-point grid, and the k-points set we used was $4 \times 4 \times 1$. In all calculations, convergence of the total energy with respect to the k-point set was confirmed. The $Rh/CeO_2(111)$ surface was modeled as 2×1 super cells. The metal-oxide slab was chosen to be three molecular CeO_2 thick, thus nine atomic layers in total, with one Rh atom on top located at an optimized position. The adsorption energy is about a 5 to 6 kcal/mol difference on the effect of the number of layers used (between 9 and 12 atomic layers). An ethanol molecule was adsorbed only on one side of this slab. The super cell has dimensions $a = 7.65$ Å, $b = 3.83$ Å, and $c = 19.80$ Å, which includes the vacuum region with a thickness ca. 12 Å to ensure that there was no interaction between the surface adsorbates of one layer and the next slab. The x and y dimensions of the unit cell were fixed at the calculated equilibrium lattice parameter for ceria bulk ($a = 5.422$ Å; experimental value, 5.411 Å;[49a] CeO_2 has a cubic structure of calcium fluorite CaF_2 type, in which the Ce atom has eight adjacent oxygen atoms[50]). To relax the surface structure, the top three atomic layers of the slab, with the adsorbates, were allowed to relax. The bottom six atomic layers were held fixed at the bulk positions of ceria. Transition states of sequential hydrogen abstraction processes and carbon−carbon bond scission were studied with the nudged elastic band (NEB) method;[51−53] according to this method, we created a linear path between the reactant and product states of each elementary process for use as an initial search coordinate and then divided the path into a series of images. Each image is optimized with respect to all nuclear degrees of freedom except the one along the reaction pathway. The transition state refers to an image for which the tangential force to the reaction path tends to zero. This approach has been shown to provide excellent convergence to saddle points on analytic potential-energy surfaces; although it employs no frequency analysis (see, for example, the ACS Symposium Series[54] for a detailed description of these analyses), the mathematics of the technique are well defined.[55,56] We also calculated the adsorption energy of H_2O in the $CeO_2(111)-(2 \times 1)$ system, and the result, $E_{ads,H_2O} = 11.80$ kcal/mol, was in good agreement with the experimental value observed by Henderson et al.[49b] (ca. 12.2 kcal/mol) in the similar system (assuming monolayer coverage of H_2O on $CeO_2(111)$ surface). Moreover, we calculated the surface energies of $CeO_2(111)$ to be 0.73 J/m^2 and made the comparison with others' works,[37−38] shown in SI (Supporting Information) Table 1. The result was quite consistent.

Results and Discussion

Our calculated results include the structure of clean Rh/CeO_2-$(111)-(2 \times 1)$ surfaces, ethanol molecule, other intermediates as gas-phase structures, $Rh/CeO_2(111)-(2 \times 1)$ surface systems with adsorbates, and the potential-energy surfaces of the possible reaction pathways; they are described in the following sections.

A. $Rh/CeO_2(111)-(2 \times 1)$ Clean Surface. The slab model for a clean $CeO_2(111)-(2 \times 1)$ surface is shown in Figure 1a, which was fully relaxed under the restriction of fixed cell parameters and the lower six layers. According to the literature,[37−39] the $CeO_2(111)$ surface relaxation is small, with the Ce sublattice remaining almost fully intact, while the O sublattice undergoes small changes of interlayer distance (∼0.03 Å) that result in a slight contraction of the few layers for the $CeO_2(111)$ surface. In the experiment performed by Imamura et al.,[23] they showed the TEM micrograph of Rh hydrosol. The hydrosol was loaded on the supports and calcined at 550 °C in

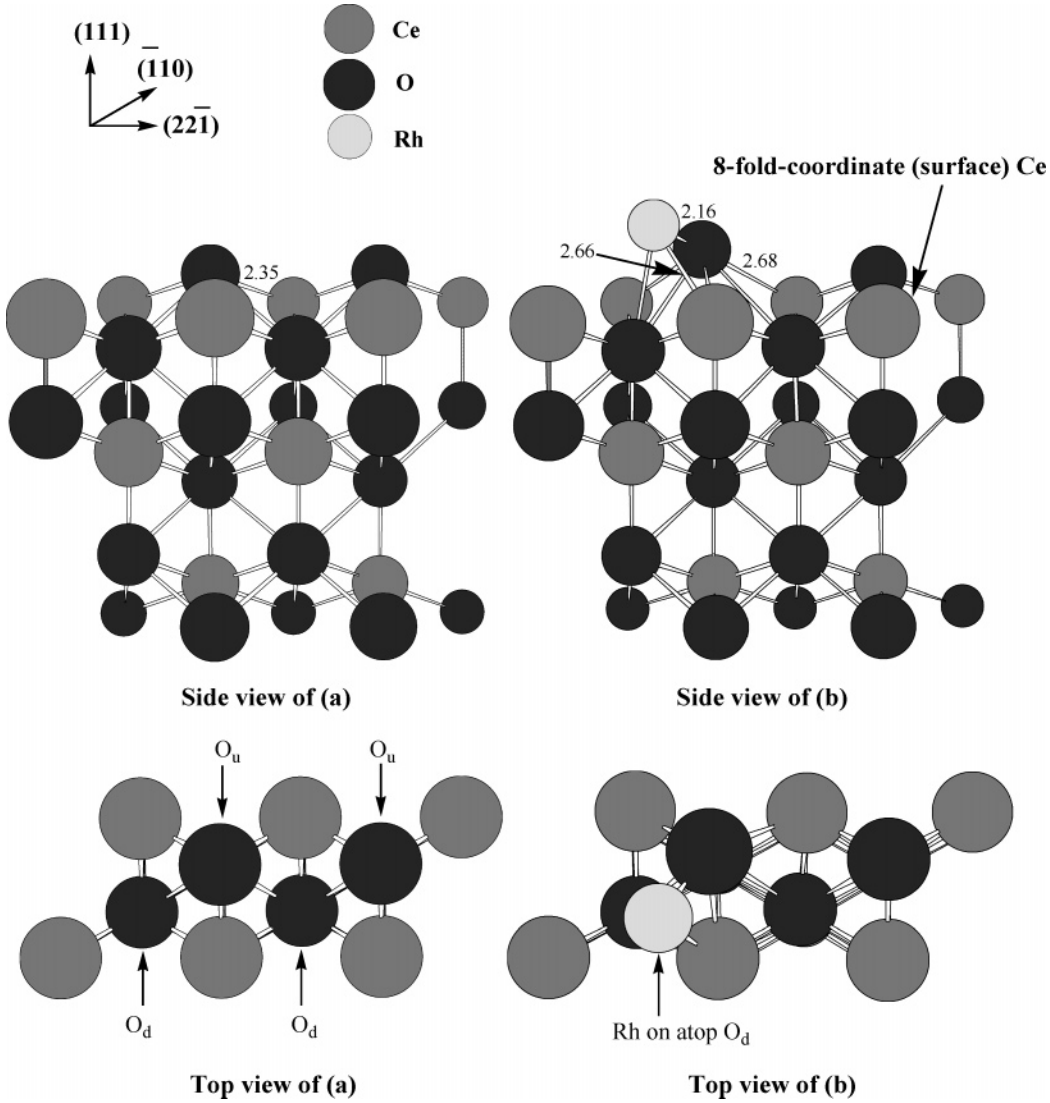

Figure 1. (a) Slab model for the ceria surface, $CeO_2(111)-(2 \times 1)$, and (b) for the Rh/CeO_2 $(111)-(2 \times 1)$ surface. The bottom six atomic layers (for both (a) and (b)) are fixed at their bulk positions, and the slabs are repeated in the z-direction with a 12 Å thick vacuum layer between slabs. O_d represents the oxygen atom locating at the down-side position while O_u represents that at the up-side position of the aforementioned structures.

air, followed by reduction at 300 °C in hydrogen. They displayed the TEM images of Rh-loaded ZnO, γ-Al_2O_3, and CeO_2, respectively, and found that the aggregation of Rh primary particles (size ranging from 30 to 80 Å) occurred on both ZnO and γ-Al_2O_3 but not on the CeO_2 counterpart, despite the fact that the presence of Rh was clearly indicated by a spot analysis using an energy-dispersive X-ray spectrophotometer (Rh, 0.619 atom % = 1.1 wt % on CeO_2). They tried every effort to obtain high-resolution electron microscope (HREM) images of Rh but all failed and finally concluded that Rh was too finely dispersed on the surface of CeO_2 to be observed by phase contrast or it had penetrated inside CeO_2 lattice. On the other hand, Rh was present as metallic particles on the surface of ceria if it were calcined at 950°C. On the basis of this evidence that the proportion of Rh exposed on the surface of ceria at low temperature (550 °C) could be small, we added only one Rh atom to our clean $CeO_2(111)-(2 \times 1)$ surface, equivalent to a surface coverage of $^1/_2$ ML (monolayer) of Rh, in our theoretical study and assumed that the ethanol-decomposition reaction occurs on this hypothetical surface. The slab model for the $Rh/CeO_2(111)-(2 \times 1)$ structure calculated to be most stable is shown in Figure 1b, in which the preferred location for the rhodium atom was atop an O_d site (where O_d represents the oxygen atom locating at the down-side position while O_u at the up-side position of the CeO_2 structure). For other possible locations (not shown here) such as atop-Ce, atop-O_u, OO-bridge, CeO-bridge, and so forth, our calculated results indicated energies about 1−2 eV greater. A significant geometric change occurs when the rhodium atom is added into the $CeO_2(111)-(2 \times 1)$ surface. The optimized distance between the added Rh atom and the surface (characterized as $Rh-O_d$) is 2.98 Å; the induced largest structural alteration is the bond length of the surface Ce−O, increased by 0.33 Å. This newly chosen $Rh/CeO_2(111)-(2 \times 1)$ surface serves as the clean model substrate.

To explore the various possible adsorption intermediates, we calculated also each single gas-phase molecule in the empty super cell. Optimized gas-phase species are shown in SI Figure 1 (species 1−10) including geometric parameters, bond lengths, and angles. The calculated electronic energies of ethanol and its fragments are listed in SI Table 2. All free, gas-phase molecules were simulated with a large unit cell of dimensions $25 \times 25 \times 25$ Å^3; the convergences were confirmed. The calculated C−C, C−O, C═C, and C═O bond lengths and the ∠CCO bond angles in all species are in satisfactory agreement with experimental values,[57−61] with the differences being insignificant, less than ±0.06 Å, and ±1.1°.

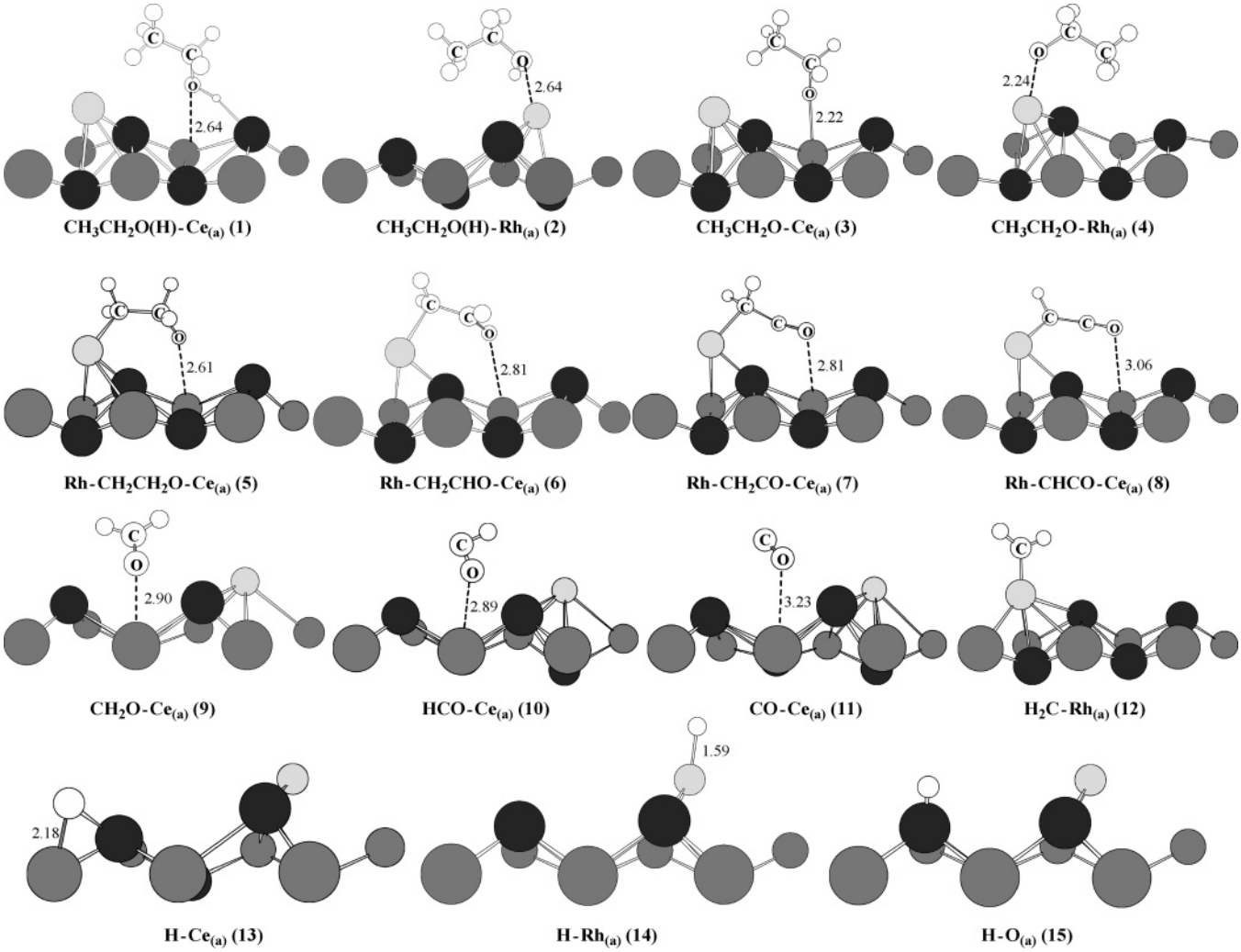

Figure 2. Calculated optimized configurations of ethanol and its fragments on the Rh/CeO_2(111)−(2 × 1) surface. The bond lengths are given in angstroms, and the H atoms are represented by the small white circles. The bottom part of the surface has been omitted, which is similar to the one shown in Figure 1.

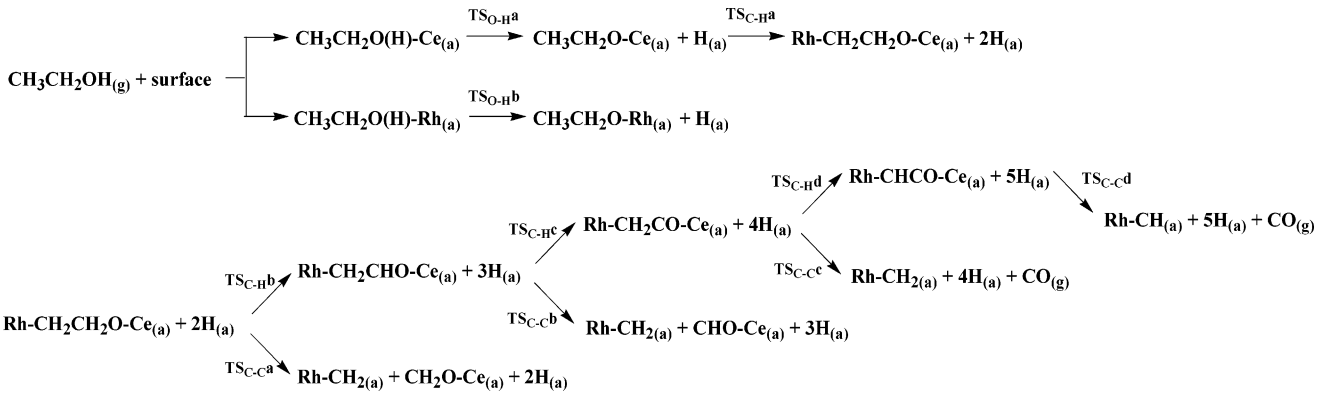

Figure 3. Proposed possible reaction schemes of ethanol on Rh/CeO_2(111)−(2 × 1) reactions.

B. Adsorption Geometries and Energetics. The dehydrogenation of ethanol and its fragments on the Rh/CeO_2(111)−(2 × 1) surface is schematically depicted in Figure 2; the optimized bond lengths and calculated adsorption energies are listed in Table 1. We began the construction of the ethanol adsorbate by adding the ethanol molecule onto the surface. The attachment of ethanol through the O atom onto the Ce atom of the surface (O···Ce) is preferable to attachment onto the Rh atom (O···Rh), as the calculated energy of physisorption for the former (13.95 kcal/mol) is greater than that for the latter (9.37 kcal/mol); the reason is likely that the carbon portion of ethanol in the former (O···Ce) construction approaches much nearer to the surface so as to enhance the surface interaction and to decrease the energy, although the distances (O···Ce) and (O···Rh) in both constructions are similar (2.64 Å), as shown in Figure 2 structures 1 and 2. We calculated also a construction with the oxygen atom of ethanol attaching to the O atom of the surface (O···O) (not shown here), which proved unstable because there is a large energy of repulsion between lone pair electrons of O and O atoms. We examined other possible

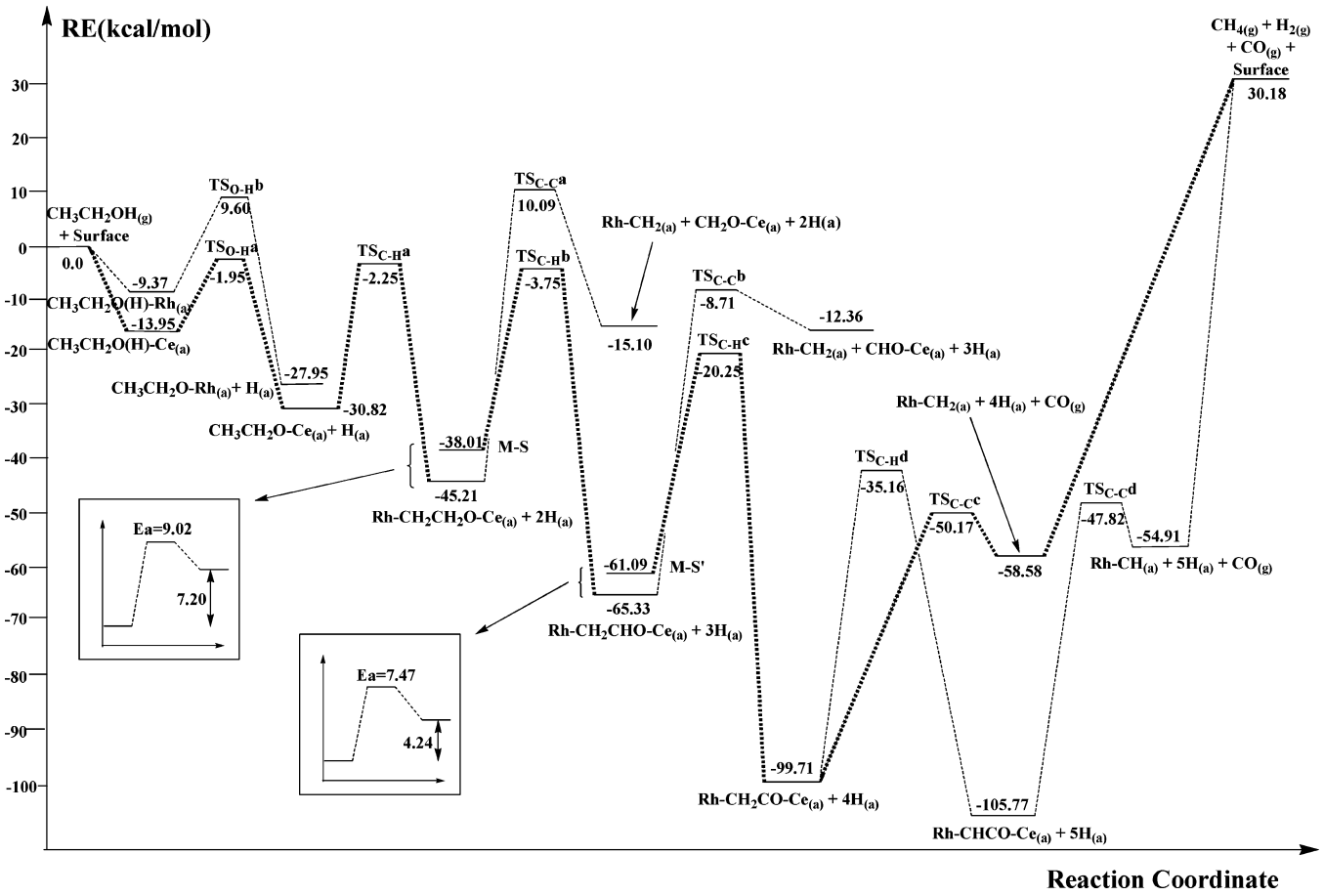

Figure 4. Calculated possible potential-energy diagram for the dehydrogenation of CH_3CH_2OH on the surface of $Rh/CeO_2(111)-(2 \times 1)$. The massive dotted line connection represents the preferable reaction pathway.

constructions involving the carbon atom of ethanol attaching to the Ce or Rh or O atom of the surface but found that no such construction was as stable as the former (O···Ce) one. A possible reason is that the saturated carbon atoms of ethanol are surrounded by hydrogen atoms that prevent the carbon atoms from direct interaction with atoms on the surface. Hence, we concluded that an initial approach of the ethanol molecule onto the $Rh/CeO_2(111)$ surface would be preferable to the (O···Ce) construction. Our calculated result shows also that the ethoxy molecule (CH_3CH_2O) prefers the (O···Ce) construction in which it is chemisorbed onto the same surface; the adsorption energy is 64.68 kcal/mol, with the O···Ce bond of length 2.22 Å, whereas the O···Rh energy is 61.81 kcal/mol and the length is 2.24 Å, shown in Table 1 and Figure 2 structures 3 and 4.

The construction of the oxirane (CH_2CH_2O) molecule as an adsorbate on the $Rh/CeO_2(111)$ surface was calculated to be stable in a six-membered ring oxametallacycle; the oxygen atom of the molecule at one end attaches to the Ce atom (O···Ce) and simultaneously the carbon atom at the other end to the Rh atom (C···Rh) of the surface, designated as $Rh-CH_2CH_2O-Ce_{(a)}$ (in which subscript (a) represents an adsorbate phase), shown in Figure 2 structure 5. This is very similar to the aforementioned five-member ring oxametallacyclic structure presented by Idriss et al.[18−22] (Idriss et al. confirmed that the five-membered-ring oxametallacyclic intermediate was a stable structure on a Rh/CeO_2 surface). Brown et al.[62,63] and Mavrikakis et al.[64,65] discovered that this construction was readily formed as an adsorption intermediate, especially for Rh-containing metal surfaces. Moreover, in homogeneous catalysis, oxametallacycles are proposed as intermediates in diverse reactions, including epoxidation and asymmetric dihydroxylation of olefins.[66,67] The sequential dehydrogenation of oxirane in this oxametallacyclic construction proceeds, and the products remain in a similar construction on the surface, such as $Rh-CH_2CHO-Ce_{(a)}$, $Rh-CH_2CO-Ce_{(a)}$, and $Rh-CHCO-Ce_{(a)}$, with substantial adsorption energies: 77.71, 50.18, and 89.80 kcal/mol, respectively, shown in Table 1 and Figure 2 structures 6, 7, and 8. In contrast, CO has a small adsorption energy, ca. 3.55 kcal/mol, with the oxygen atom attaching to the Ce atom of the surface. The optimized (O···Ce) distance is 3.23 Å, too large to be held stable on the surface, shown in Figure 2 structure 11, in good accord with the result from Yang et al. [39] in which they found the adsorption energy to be much weaker (ca. 3.92 kcal/mol), no matter which end of the molecule (C or O end) faces the CeO_2-(111) surface. In contrast, the CH_2 fragment attaches tightly in a (C···Rh) construction with a large adsorption energy (92.13 kcal/mol) and much smaller (C···Rh) distance (1.80 Å), as shown in Figure 2 structure 12. The possible reasons are discussed in subsequent sections. We investigated also the adsorption energy of an H atom onto the surface. Three possible adsorption constructions—(H···Ce), (H···Rh), and (H···O)—are shown in Figure 2 structures 13, 14, and 15, with adsorption energies and bond lengths calculated to be 28.52 kcal/mol and 2.18 Å, 56.25 kcal/mol and 1.59 Å, and 101.59 kcal/mol and 0.97 Å, respectively. The hydrogen atom detached from ethanol or another fragment would preferably adsorb onto the oxygen atom (H···O) of the CeO_2 surface. This result agrees with that of Wang et al.,[68] for which they calculated the hydrogen adsorption energy onto the TiO_2 surface of (H···O) construction

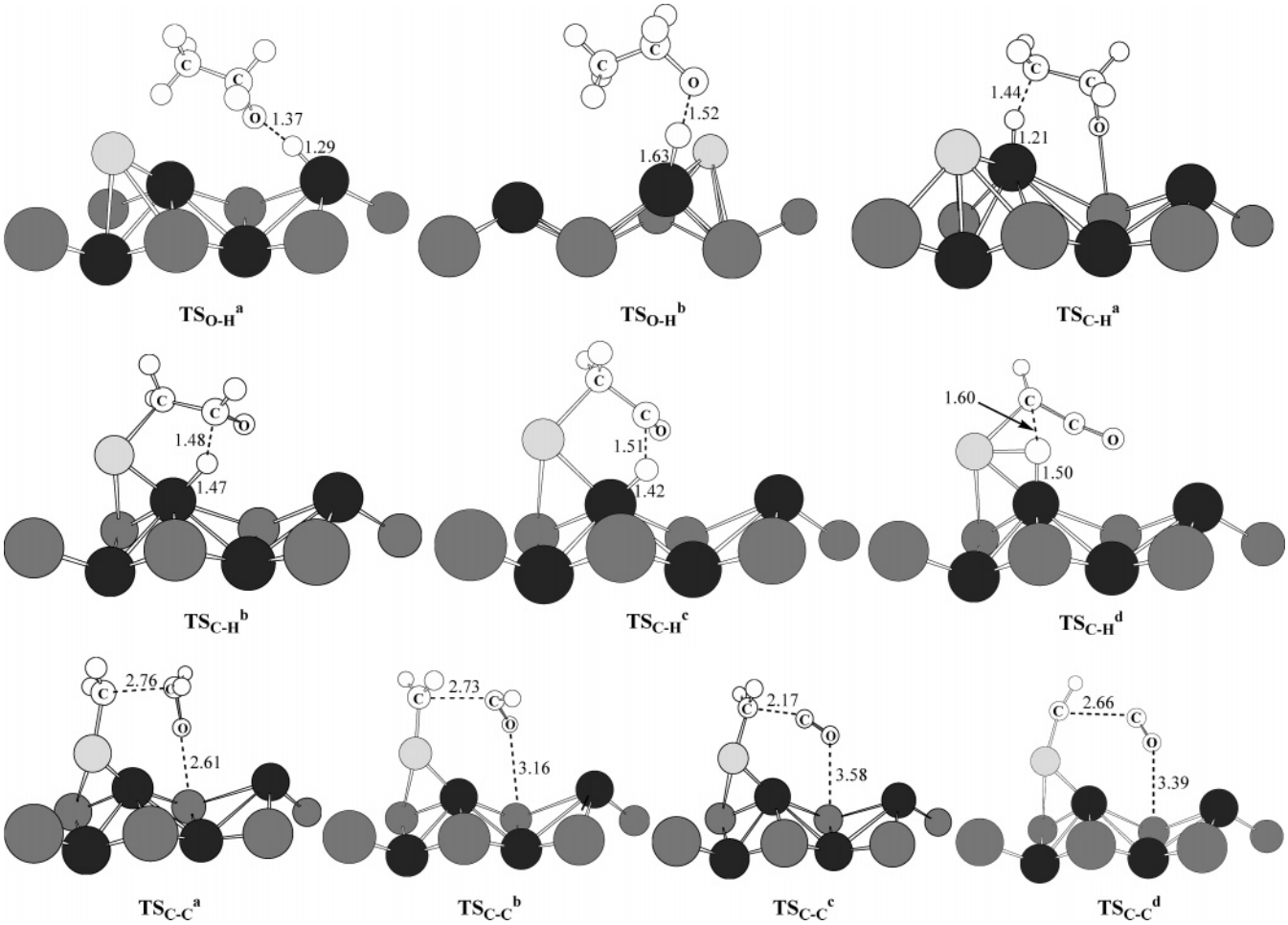

Figure 5. Optimized configuration of the calculated transition structures by using NEB method. The bond lengths are given in angstroms, and the H atoms are represented by the small white circles. The bottom part of the surface has been omitted, which is similar to the one shown in Figure 1.

SCHEME 2

$C_{(g)} \longrightarrow A_{(g)} + B_{(g)}$	ΔE = x kcal/mol	(*gas phase reaction*)
$A_{(g)} \longrightarrow A_{(a)}$	ΔE = y kcal/mol	(*adsorption*)
$B_{(g)} \longrightarrow B_{(a)}$	ΔE = z kcal/mol	(*adsorption*)
$C_{(a)} \longrightarrow C_{(g)}$	ΔE = g kcal/mol	(*desorption*)
$C_{(a)} \longrightarrow A_{(a)} + B_{(a)}$	$\Delta E_{overall}$ = (x+y+z+g) kcal/mol	(*net reaction energy*)

to be 118 kcal/mol, greater than (H···Ti), with a (H···O) bond distance 0.965 Å.

C. Potential-energy Surfaces. The proposed possible subsequent pathways for dehydrogenation of ethanol on a Rh/CeO_2-(111) surface are schematically depicted in Figure 3; the calculated corresponding potential-energy surfaces are drawn in Figure 4, and the possible transition structures are drawn in Figure 5. We describe the dehydrogenation scheme by splitting it into two parts—from ethanol adsorbate to the formation of an oxametallacyclic complex $Rh-CH_2CH_2O-Ce_{(a)}$ and from $Rh-CH_2CH_2O-Ce_{(a)}$ to the ultimate products. The overall reaction energy for a particular step is calculated by constructing a Haber cycle according to Scheme 2. The calculated adsorption energies of the reactants and products along with the gas-phase reaction energy can be used to calculate the surface reaction energy.

C-1 Formation of $Rh-CH_2CH_2O-Ce_{(a)}$. As the adsorption energies of two possible constructions of ethanol adsorbate on the $Rh/CeO_2(111)$ surface, $CH_3CH_2O(H)-Ce_{(a)}$ and $CH_3CH_2O(H)-Rh_{(a)}$, are similar, 13.95 vs 9.37 kcal/mol, we performed a calculation for dehydrogenation of the O−H bond in each construction. The transition states of the first dehydrogenation of $CH_3CH_2O(H)-Ce_{(a)}$ and $CH_3CH_2O(H)-Rh_{(a)}$, producing $CH_3CH_2O-Ce_{(a)}$ and $CH_3CH_2O-Rh_{(a)}$, respectively, were located by a series of elastic bands using the NEB method.[51−53] The calculated transition barrier for the former, 12.00 kcal/mol, is much smaller than that for the latter, 18.97 kcal/mol. Both energies indicate the existence of a large surface-catalytic effect for the dehydrogenation of the O−H bond on the Rh/CeO_2-(111) surface relative to the similar process in the gaseous phase, 104.1 kcal/mol.[22] Besides, the dehydrogenation product $CH_3-CH_2O-Ce_{(a)}$ is more stable by 2.87 kcal/mol than the $CH_3-CH_2O-Rh_{(a)}$ counterpart. In addition, comparison of the O−H distance in these two calculated transition structures, shown in Figure 5, makes clear that $r_{(H-O(Ce))} = 1.37$ Å is smaller than $r_{(H-O(Rh))} = 1.52$ Å. According to the Hammond postulate,[69] the former process, via $TS_{(H-O(Ce))}$, would not only have a lower energy barrier but also release more heat to attain the following product. That is, $CH_3CH_2O-Ce_{(a)}$ becomes more stable than $CH_3CH_2O-Rh_{(a)}$, in agreement with our calculation. We thus predict that the first dehydrogenation of ethanol adsorbate occurs as $CH_3CH_2O(H)-Ce_{(a)} \rightarrow CH_3CH_2O-Ce_{(a)} + H_{(a)}$. Then, scission of the β-carbon hydrogen bond occurs via the transition structure TS_{C-H}^{a}, to form a stable six-membered ring oxametallacycle, $Rh-CH_2CH_2O-Ce_{(a)}$. The barrier is calculated to be 28.57 kcal/mol, also much smaller than a typical energy, 93.3 kcal/mol,[22] to break a C−H bond without a surface catalytic

effect. Atherton et al.[70,71] reported that Rh metal was known to activate the C−H bond; the Rh/CeO_2 surface thus accelerated the H_2C-H scission and released the H atom to the surface. We found that the interaction between the Rh atom and the β-CH_2 fragment was so strong—with the calculated adsorption energy of $H_2C-Rh_{(a)}$ being 92.13 kcal/mol—that it favored the formation of a $Rh-CH_2CH_2O-Ce_{(a)}$ oxametallacycle, predicted and observed by several authors.[18−22,62−67]

C-2 from $Rh-CH_2CH_2O-Ce_{(a)}$ to Final Products. Our prediction for the possible reaction pathway is either dehydrogenation from the α-carbon hydrogen, or scission of the carbon−carbon bond. The former process involves the formation of another oxametallacyclic adsorbate, $Rh-CH_2CHO-Ce_{(a)}$, but in the initial state, $Rh-CH_2CH_2O-Ce_{(a)}$, of this pathway the carbon−hydrogen atom is away from the surface, which makes abstraction of the H atom (dehydrogenation) onto the surface too difficult. Rotating the C−H bond leaves it more near to the $Rh/CeO_2(111)$ surface, in another local minimum, metastable state, about 7.20 kcal/mol higher, shown as M−S in Figure 4, which substantially decreases the dehydrogenation barrier. As shown in the figure, there is a connection between the initial state and the M−S with a small transition barrier, 9.02 kcal/mol, and the dehydrogenation barrier (TS_{C-H}^{b}) becomes greatly diminished, as small as 34.26 kcal/mol. For scission of the carbon−carbon bond from $Rh-CH_2CH_2O-Ce_{(a)}$ to form $Rh-CH_{2(a)}$ and $CH_2O-Ce_{(a)}$, the barrier is large, 55.30 kcal/mol. This pathway is, moreover, endothermic, with $\Delta H = 30.11$ kcal/mol, relative to the former dehydrogenation process, which is exothermic with $\Delta H = -27.32$ kcal/mol. One can hence predict the third dehydrogenation to be preferable to scission of the carbon−carbon bond. A similar situation is encountered for the succeeding intermediate adsorbate, $Rh-CH_2CHO-Ce_{(a)}$, for which the dissociation of the other α-carbon hydrogen would compete with scission of the carbon−carbon bond. We located another metastable state, M−S′, to initiate dissociation of the C−H bond, having a barrier, TS_{C-H}^{c}, 40.84 kcal/mol, and releasing much heat, −38.62 kcal/mol, to form another intermediate adsorbate, $Rh-CH_2CO-Ce_{(a)}$. In contrast, the barrier for endothermic scission of the carbon−carbon bond, TS_{C-C}^{b}, to form $Rh-CH_{2(a)}$ and $CHO-Ce_{(a)}$ is much greater, 56.62 kcal/mol. The fourth dehydrogenation would thus occur before scission of the carbon−carbon bond. On which of these pathways the $Rh-CH_2CO-Ce_{(a)}$ adsorbate would occur became a major concern; our calculation shows that the barrier to dissociate the C−H bond of the β-carbon to form $Rh-CHCO-Ce_{(a)}$ is much greater, 64.55 kcal/mol (TS_{C-H}^{d}). We were initially unable to find a connected metastable state to decrease the barrier in this $Rh-CH_2CO-Ce_{(a)}$ adsorbate. In contrast, the barrier for scission of the carbon−carbon bond to form $Rh-CH_{2(a)}$ and $CO_{(g)}$ is smaller than that in previous predictions, only 49.54 kcal/mol for TS_{C-C}^{c}, even much smaller (about 15 kcal/mol less) than dehydrogenation at the β-carbon. The optimized transition structure shows the Ce−OC distance to be 3.58 Å; we thus predict that CO would desorb readily from the surface at this stage. Upon comparing the transition structure of TS_{C-H}^{d} with other C−H bond dissociation counterparts (in Figure 5), we discovered that the C−H distance, 1.60 Å, in TS_{C-H}^{d} is much greater than those in TS_{C-H}^{b}, 1.48 Å, and TS_{C-H}^{c}, 1.51 Å. According to the Hammond postulate, it is reasonable to predict a greater barrier in TS_{C-H}^{d}. The same postulate is applicable to the TS_{C-C}^{c} barrier being smaller than analogous carbon−carbon scissions. The carbon−carbon distance in TS_{C-C}^{c} is only 2.17 Å, much smaller than those in TS_{C-C}^{a}, 2.76 Å, and TS_{C-C}^{b}, 2.73 Å. We hence predicted that scission of the carbon−carbon bond would occur at this stage, to form $Rh-CH_{2(a)}$ and $CO_{(g)}$, despite the fifth dehydrogenation to form $Rh-CHCO-Ce_{(a)}$ adsorbate being exothermic. We also performed a calculation for other possible pathways following the formation of $Rh-CHCO-Ce_{(a)}$ adsorbate but found neither a stable dehydrogenation product, $Rh-CCO-Ce_{(a)}$, nor a transition structure beyond the pathway involving scission of the carbon−carbon bond to form $Rh-CH_{(a)}$ and $CO_{(g)}$. The calculated barrier is 57.95 kcal/mol for TS_{C-C}^{d}, larger than that for TS_{C-C}^{c}, implying that scission of the carbon−carbon bond would be favored to occur at the $Rh-CH_2CO-Ce_{(a)}$ stage.

As desorption processes, such as reactions $H_{(a)} + H_{(a)} \rightarrow H_{2(g)}$ and $CH_{2(a)} + 2H_{(a)} \rightarrow CH_{4(g)}$, are known to be driven by a large entropy term at elevated temperatures, the endothermic nature of the final step presents no significant problem. This result is in agreement with Idriss et al.[19] who proposed the same final products: $H_{2(g)}$, $CO_{(g)}$, and $CH_{4(g)}$.

Conclusion

With periodic DFT calculations, we investigated the thermochemistry and reaction barriers of ethanol dehydrogenation on a $Rh/CeO_2(111)$ surface. The most likely pathway for dehydrogenation involves the formation of an oxametallacyclic compound, $Rh-CH_2CH_2O-Ce_{(a)}$, followed by sequential α-carbon hydrogen abstractions forming $Rh-CH_2CHO-Ce_{(a)}$, $Rh-CH_2CO-Ce_{(a)}$, and eventually scission of the C−C bond. The smallest energy barrier in this pathway is the initial scission of the ethanol O−H bond, ca. 12 kcal/mol, followed by dissociation of a β-C−H bond, ca. 28 kcal/mol, to form the oxametallacyclic $Rh-CH_2CH_2O-Ce_{(a)}$. Our calculation shows that scission of the C−C bond occurs at the $Rh-CH_2CO-Ce_{(a)}$ stage, which has the smallest barrier, ca. 50 kcal/mol, for dissociation of the C−C bond, compared with other stages, and forms desorbed $CO_{(g)}$. The calculated energetic data of all reaction intermediates including the transition states along this pathway, up to the formation of $Rh-CH_{2(a)} + CO_{(g)}$, are below the starting reference point, $CH_3CH_2OH_{(g)}$ + surface, indicating a free supplement of thermal energy for the reaction to proceed to this point. Transfer of heat to the system is, however, essential for desorption of molecular hydrogen and other products. As the dehydrogenation barriers of ethanol and its fragments on the Rh/CeO_2 surface appear not to have been reported either experimentally or theoretically, our results represent the estimates of barriers of these possible kinds in our assumed Rh/CeO_2 surface.

Acknowledgment. This research was supported by the Institute of Nuclear Energy Research, Atomic Energy Council, Taiwan (ROC), under Contract No. NL940251. We are deeply indebted to Professor M. C. Lin from NCTU in Taiwan for his persistent encouragement and instruction. We are also grateful to the National Center for High-Performance Computing where the computer time was provided. We want to thank Professor J. C. Jiang and Professor M. Hayashi, as well as H. T. Chen and C. L. Huang for their useful discussion.

Supporting Information Available: Figure showing calculated gas-phase species using the VASP package, and tables giving a comparison of calculated surface energies and calculated electronic total energies for gas-phase ethanol and its fragments. This material is available free of charge via the Internet at http://pubs.acs.org.

References and Notes

(1) Dresselhaus, M. S.; Thomas, I. L. *Nature* **2001**, *414*, 332.

(2) Hibino, T.; Hashimoto, A.; Inoue, T.; Tokuno, J. I.; Yoshida, S. I.; Sano, M. *Science* **2000**, *288*, 2031. (b) Park, S.; Vohs, J. M.; Gorte, R. J. *Nature* **2000**, *404*, 265. (c) Steele, B. C. H.; Heinzel, A. *Nature* **2001**, *414*, 345.

(3) Trovarelli, A. *Catal. Rev. Sci. Eng.* **1996**, *38*, 439.

(4) Kaspar, J.; Fornasiero, P.; Graziani, M. *Catal. Today* **1999**, *50*, 285.

(5) Trovarelli, A. *Catal. Rev. Sci. Eng.* **1996**, *38*, 439. (b) Rodriguez, J. A.; Wang, X.; Hanson, J. C.; Liu, G.; Iglesias-Juez, A.; Ferna'ndez-Garcý'a, M. *J. Chem. Phys.* **2003**, *119*, 5659. (c) Rodriguez, J. A. *Catal. Today* **2003**, *85*, 177.

(6) Taylor, K. C. *Catal. Rev. Sci. Eng.* **1995**, *35*, 457.

(7) *Basic Research Needs for Vehicles of the Future*; Eisenberger, P. M., Ed; Princeton Materials Institute: Princeton, NJ, 1995.

(8) Yao, H. C.; Yao, Y. F. Y. *J. Catal.* **1984**, *86*, 254.

(9) Taylor, K. C. *Proceedings of Catalytic and Automotive Pollution Control*; Brussels, Belgium, 1986.

(10) Fisher, G. B.; Thesis, J. R.; Casarella, M. V.; Mahan, S. T. *SAE Technol. Pap. Ser.*; No. 931034, 1993.

(11) Stubenrauch, J.; Vohs, J. M. J. *J. Catal.* **1996**, *159*, 50.

(12) Kundakovic, L.; Stephanopoulos, M. F. *J. Catal.* **1998**, *179*, 203. (b) Tiernan, M. J.; Fimlayson, O. E. *Appl. Catal., B* **1998**, *19*, 23.

(13) Liu, W.; Stephanopoulos, M. F. *J. Catal.* **1995**, *153*, 304 and 317. (b) Dictor, R.; Roberts, S. *J. Phys. Chem.* **1989**, *93*, 5846.

(14) Zaki, M. I.; Hasan, M. A.; Pasupulety, L. *Langmuir* **2001**, *17*, 768. (b) Idriss, H.; Diagne, C.; Hindermann, J. P.; Kiennemann, A.; Barteau, M. A. *J. Catal.* **1995**, *155*, 219.

(15) Whittingham, M. S.; Savinell, R. F.; Zawodzinski, T. *Chem. Rev.* **2004**, *104*, 4243.

(16) Holladay, J. D.; Wang, Y.; Jones, E. *Chem. Rev.* **2004**, *104*, 4767.

(17) Logan, B. E. *Environ. Sci. Technol.* **2004**, *38*, 160A.

(18) Yee, A.; Morrison, S. J.; Idriss. H. *Catal. Today* **2000**, 63, 327.

(19) Sheng, P.-Y.; Yee, A.; Bowmaker, G. A.; Idriss, H. *J. Catal.* **2002**, *208*, 393.

(20) Sheng, P.-Y.; Bowmaker, G. A.; Idriss, H. *Appl. Catal. A* **2004**, *261*, 171.

(21) Sheng, P. Y.; Idriss, H. *J. Vac. Sci. Technol., A* **2004**, *22*, 1652.

(22) Idriss, H. *Platinum Met. Rev.* **2004**, *48*, 105.

(23) Imamura, S.; Yamashita, T.; Hamada, R.; Saito, Y.; Nakao, Y.; Tsuda, N. *J. Mol. Catal. A: Chem.* **1998**, *129*, 249.

(24) Liguras, D. K.; Goundani, K.; Verykios, X. E. *J. Power Sources* **2004**, *130*, 30.

(25) Fatsikostas, A. N.; Kondarides, D. I.;. Verykios, X. E. *Catal. Today* **2002**, *75*,145.

(26) Garcia, E.; Laborde, M. *Int J. Hydrogen Energy* **1991**, *16* (5), 307.

(27) Vasudeva, K.; Mitra, N.; Umasankar, P.; Dhingra, S. *Int J. Hydrogen Energy* **1996,** *21* (1), 13.

(28) Fishtik, I.; Alexander, A.; Datta, R.; Geana, D. *Int J. Hydrogen Energy* **2000**, *25*, 31.

(29) Haga, F.; Nakajima, T.; Mishima, S. *Catal. Lett.* **1997**, *48*, 223.

(30) Cavallaro, S.; Freni, S. *Int J. Hydrogen Energy* **1996**, *21* (6), 465.

(31) Cavallaro, S.; Mondello, N.; Freni, S. *J. Power Sources* **2001,** *102*, 198.

(32) Aupretre, F.; Descorme, C.; Duprez, D. *Catal. Commun.* **2002,** *3*, 263.

(33) Breen, J.; Burch, R.; Coleman, H. *Appl. Catal. B* **2002**, *39*, 65.

(34) Freni, S. *J. Power Sources* **2001,** *94*, 14.

(35) Liguras, D. K.; Kondarides, D. I.; Verykios, X. E. *Appl. Catal. B* **2003**, *43*, 345.

(36) Skorodumova, N. V.; Simak, S. I.; Lundqvist, B. I.; Abrikosov, I. A.; Johansson, B. *Phys. Rev. Lett.* **2002**, *89*, 166601.

(37) Skorodumova, N. V.; Baudin, M.; Hermansson, K. *Phys. Rev. B* **2004**, *69*, 075401.

(38) Yang, Z.; Woo, T. K.; Baudin, M.; Hermansson, K. *J. Chem. Phys.* **2004**, *120*, 7741.

(39) Yang, Z.; Woo, T. K.; Hermansson, K. *Chem. Phys. Lett.* **2004**, *396*, 384.

(40) Gennard, S.; Cora, F.; Catlow, C. R. A. *J. Phys. Chem. B* **1999**, *103*, 10158.

(41) Siokou, A.; Nix, R. M. *J. Phys. Chem. B* **1999**, *103*, 6984.

(42) Kresse, G.; Hafner, J. *Phys. Rev. B* **1993**, *47*, 558.

(43) Kresse, G.; Furthmuller, J. *Comput. Mater. Sci.* **1996**, *6*, 15.

(44) Kresse, G.; Hafner, J. *Phys. Rev. B* **1996**, *54*, 169.

(45) White, J. A.; Bird, D. M. *Phys. Rev. B* **1994**, *50*, 4954.

(46) Perdew, J. P.; Chevary, J. A.; Vosko, S. H.; Jackson, K. A.; Pederson, M. R.; Singh, D. J.; Fiolhais, C. *Phys. Rev. B* **1992**, *46*, 6671.

(47) Blochl, P. E. *Phys. Rev. B* **1994**, *50*, 17953. (b) Kresse, G.; Joubert, D. *Phys. Rev. B* **1999**, *59*, 1758.

(48) Clotet, A.; Pacchioni, G. *Surf. Sci.* **1996**, *346*, 91.

(49) Sellars, H. *J. Phys. Chem.* **1990**, *94*, 8329. (b) Henderson, M. A.; Perkins C. L.; Engelhard, M. H.; Thevuthasan, S.; Peden, C. H. F. *Surf. Sci.* **2003**, *526*, 1.

(50) *The Oxide Hanbook*; Samsonov, G. V., Ed.; IFI/Plenum: New York, 1982.

(51) Ulitsky, A.; Elber, R. *J. Chem. Phys.* **1990**, *92*, 1510.

(52) Mills, G.; Jo'nsson, H.; Schenter, G. K. *Surf. Sci.* **1995**, *324*, 305.

(53) Henkelman, G.; Uberuaga, B. P.; Jo'nsson, H. *J. Chem. Phys.* **2000**, *113*, 9901.

(54) Truhlar, D. G.; Morokuma, K. *Transition State Modeling for Catalysis*; Oxford University Press: Washington, DC, 1999; Vol. 721, p 521.

(55) Henkelman, G.; Jo'nsson, H. *J. Chem. Phys.* **1999**, *111*, 7010.

(56) Henkelman, G.; Jo'nsson, H. *J. Chem. Phys.* **2000**, *113*, 9978.

(57) Lide, D. R., Ed. In *CRC Handbook of Chemistry and Physics*, 3rd electronic ed.; CRC Press: Boca Raton, FL, 2000.

(58) Sosa, C.; Schlegel, H. B. *J. Am. Chem. Soc.* **1987**, *109*, 7007.

(59) Kuwata, K. T.; Hasson, A. S.; Dickinson, R. V.; Petersen, E. B.; Valin, L. C. *J. Phys. Chem. A* **2005**, *109*, 2514.

(60) Tokmakov, I. V.; Moskaleva, L. V.; Paschenko, D. V.; Lin, M. C. *J. Phys. Chem. A* **2003**, *107*, 1066.

(61) Dixon, D. A.; Feller, D.; Francisco, J. S. *J. Phys. Chem. A* **2003**, *107*, 186.

(62) Brown, N. F.; Barteau, M. A. *Surf. Sci.* **1993**, *298*, 6.

(63) Brown, N. F.; Barteau, M. A. *Langmuir* **1995**, *11*, 1184.

(64) Mavrikakis, M.; Doren, D. J.; Barteau, M. A. *J. Phys. Chem.* **1998**, *102*, 394.

(65) Jones, G. S.; Mavrikakis, M.; Barteau, M. A.; Vohs, J. M. *J. Am. Chem. Soc.* **1998**, *120*, 3196.

(66) Jorgensen, K. A.; Schiott, B. *Chem. Rev.* **1990**, *90*, 1483.

(67) Zlota, A. A.; Frolow F.; Milstein D. *J. Am. Chem. Soc.* **1990**, *112*, 6411.

(68) Wang, J.-H.; Lin, M. C.; Sun, Y.-C. *J. Phys. Chem. B* **2005**, *109*, 5133.

(69) Hammond, G. S. *J. Am. Chem. Soc.* **1955**, *77*, 334.

(70) Atherton, M. J.; Fawcett, J.; Holloway, J. H.; Hope, E. G.; Karacar, A.; Russell, D. R.; Saunders, G. C. *J. Chem. Soc., Dalton Trans.* **1996**, *15*, 3215.

(71) Atherton, M. J.; Fawcett, J.; Holloway, J. H.; Hope, E. G.; Martin, S. M.; Russell, D. R.; Saunders, G. C. *J. Organomet. Chem.* **1998**, *555*, 67.